Electronic Coupling in Mixed-Valence Dinuclear Ferrocenes and Cobaltocenes with Saturated Bridging Groups

Simon C. Jones,[a, b] Stephen Barlow,*[b] and Dermot O'Hare*[a]

Abstract: We have synthesised a series of new dinuclear metallocenes [{M-(Cp*)(C$_5$H$_4$)}$_2$X] (Cp* = η^5-pentamethylcyclopentadienyl; M = Fe, Co, X = CMe$_2$, SiMe$_2$, GeMe$_2$; M = Fe, X = Si$_2$Me$_4$). For the neutral dicobalt complexes, magnetic susceptibility measurements reveal intramolecular antiferromagnetic interactions of −21 and −14 cm^{-1} for SiMe$_2$- and GeMe$_2$-bridged species, respectively, but negligible interaction for the CMe$_2$-bridged compound. In contrast, intervalence charge-transfer (IVCT) data for the

Keywords: electron transfer · electronic coupling · metallocenes · mixed-valent compounds · through-space interactions

mixed-valence monocations of both Fe and Co complexes show electronic coupling to decrease in the order CMe$_2$ > SiMe$_2$ > GeMe$_2$. This suggests that electronic coupling is principally through-space in contrast to results found from previous studies. The IVCT data also show much stronger coupling in the dicobalt species versus their diiron analogues.

Introduction

Mixed-valence (MV) compounds can be regarded as simple systems for testing electron-transfer models; analysis of their charge-transfer spectra in the context of Marcus theory was first outlined by Hush in 1967.[1] Complexes featuring linked ferrocenium/ferrocene redox centres represent one of the most widely investigated families of MV systems; a plethora of species built around an extensive range of bridging groups have been studied in detail by variety of techniques.[2] However, there is still a paucity of studies on analogous cobaltocenium/cobaltocene systems, even though evidence exists that greater electronic coupling between the metal centres should be a feature of the Co species; this may reflect to some extent synthetic issues encountered that

have their origin in the greater chemical sensitivity of cobaltocenes when compared to ferrocenes. The relative rates of self-exchange for the [Co(Cp$'$)$_2$]$^+$/[Co(Cp$'$)$_2$] couples (Cp$'$ = Cp, Cp*) in a given solvent are greater by around an order of magnitude than for the respective Fe species;[3–5] gas-phase measurements[6] also reveal a substantial increase in rate for the Co couples in the absence of any solvent effects. These Fe and Co redox couples have been reported to have similar reorganisation energies,[3] and so the difference in self-exchange rates has been interpreted as arising from stronger through-space intermolecular coupling in the Co case. This is due to the nature of the frontier orbitals involved in the electron-transfer process. For Fe, INDO-SCF calculations[7] show the HOMO is the e$_2$ orbital, which has 86% metal character. For Co, the e$_1$* orbital is involved; Xα calculations[8] show this orbital has significant ligand character (43%), a result supported by EPR measurements on cobaltocene.[9] The active orbitals for the Co couple are, therefore, substantially delocalised onto the ligand and, hence, larger donor–acceptor orbital overlap is possible, leading to greater electronic coupling and a faster rate of electron transfer than for the Fe couple. This self-exchange process is analogous to thermal intervalence charge transfer (IVCT) in a symmetric MV complex. Limited results for MV complexes suggest a greater degree of metal–metal coupling in cobaltocenium/cobaltocene systems than for the ferrocenium/ferrocene analogues, although the majority of these studies have been carried out in strongly coupled species at, or close to, the Class III (delocalised) regime.[10] Investiga-

[a] Dr. S. C. Jones, Prof. D. O'Hare
Chemistry Research Laboratory, Department of Chemistry
University of Oxford, Mansfield Rd, Oxford, OX1 3TA (UK)
Fax: (+44) 1865-285-131
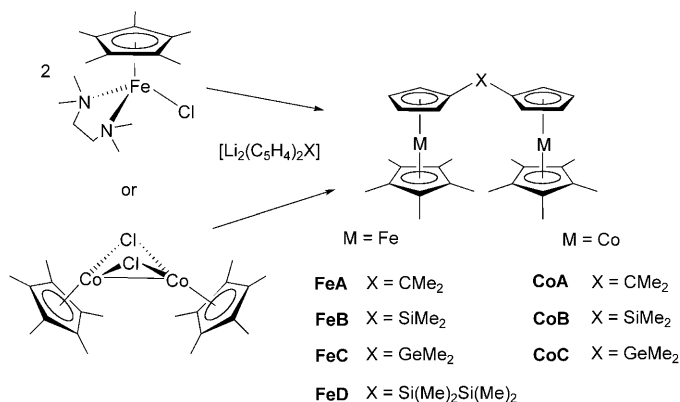E-mail: dermot.ohare@chem.ox.ac.uk

[b] Dr. S. C. Jones, Dr. S. Barlow
School of Chemistry and Biochemistry
Georgia Institute of Technology, Atlanta, GA 30332 (USA)
Fax: (+1) 404-894-5909
E-mail: stephen.barlow@chemistry.gatech.edu

Supporting information for this article is available on the WWW under http://www.chemeurj.org/ or from the author. The experimental details of the crystallographic measurements are provided in the Supporting Information along with other material as described in the text.

tion of the IVCT band for the bimetallocene monocations, $[\{M(Cp)\}_2(\mu\text{-}Fv)]^+$ ($Fv = $ fulvalenediyl, $\eta^5\!:\!\eta^5\text{-}C_{10}H_8$), shows that the bicobaltocene species is at least Class II–III, whereas the biferrocene cation is Class II.[11] IVCT spectra of Class III ligand-bridged dinuclear monocations (in which the ligand is Fv,[11] s-indacene or pentalene)[12] also show greater electronic coupling for the Co species than their Fe analogues. Studies of Fe^{II}/Fe^{I} MV species (isoelectronic with Co^{III}/Co^{II}) provide corroborating evidence for this orbital effect on electronic coupling. $[\{Fe(\eta^6\text{-}C_6Me_6)\}_2(\mu\text{-}Fv)]^+$ $[BF_4]^-$ is shown to be delocalised on both Mössbauer and IR timescales (and thus Class III),[13] whereas $[\{Fe(Cp^*)_2\}(\mu\text{-}Fv)]^+[I_3]^-$ is localised on both IR and Mössbauer timescales with separate Fe^{II} and Fe^{III} centres distinguishable in its crystal structure.[14] However, at the weak coupling (Class I/ Class II) end of the MV spectrum there are no direct comparisons for structurally analogous linked ferrocene and cobaltocene systems. Recent studies resulted in the observation of the electronic coupling (V) in the range 371–1049 cm^{-1} for *unsymmetrical* methylene-bridged Co^{III}/Fe^{II} systems,[15] whilst $[Fc_2CH_2]^+$ ($Fc = Fe(Cp)(\eta^5\text{-}C_5H_4)$) was reported to show no IVCT transition and only weak coupling ($V = 24$ cm^{-1}) was detected for $[Fc_3CH]^+$.[16] Here we have designed a series of dinuclear metallocenes linked with saturated bridging groups for which *both* Fe and Co examples are synthetically accessible. This allows investigation of electronic coupling in directly comparable Fe and Co systems towards the weakly coupled limit for the first time.

Results and Discussion

Synthesis and characterisation: Reaction of a "half-sandwich" source of "$[M(Cp^*)]^+$" ($M = Fe, Co$) with the dilithium salt of the respective ligand afforded the dinuclear metallocenes **FeA–FeD** and **CoA–CoC** (Scheme 1), which were characterised by NMR spectroscopy, mass spectrometry and elemental analysis; surprisingly $[Fe(Cp^*)Cl(tmeda)]$ has received little attention as a "half-sandwich" reagent[17–19] despite its ease of preparation when compared to the notoriously capricious $[Fe(Cp^*)(acetylacetonate)]$.[20,21] As expect-

ed, the cobaltocenes are air-sensitive, while the ferrocenes are air-stable materials. Sharp ^1H NMR spectra were resolvable for all of these compounds, even though the cobaltocenes contain unpaired electrons (vide infra); for the Co complexes certain resonances do, however, display significant paramagnetic shifts (see Supporting Information for a typical ^1H NMR spectrum). Similarly well-resolved ^1H NMR spectra have been described in the literature for other cobaltocenes.[22–24] Single crystals of **CoA**, **CoB** and **FeC** were grown from Et_2O. The structure of **CoB** is shown in Figure 1a; **CoA** and **FeC** are essentially isostructural and are depicted in the Supporting Information along with geometric details for all three structures. The bond lengths and angles of the constituent metallocene units are typical for Fe or Co metallocenes. These metallocene units have a transoid configuration with respect to the bridging ligand in all three structures; conformation of species such as these may be described by the torsion angles, ψ and φ, as illustrated in Figure 1b (the torsion angle is defined between the metal–$C_{Cp,bridge}$, $C_{Cp,bridge}$–E_{bridge} and E_{bridge}–$C_{Cp,bridge}$ bonds). Previous molecular mechanics studies of similar dimeric and oligomeric metallocene species in the gas phase[25,26] suggest that conformational preference is determined by competition between inter- and intramolecular $Cp\cdots M$ electrostatic interactions, often resulting in one or more of the torsion angles between metallocene units being significantly less than 180°. For **CoA**, **CoB** and **FeC**, both of the torsion angles are very close to 180°, presumably indicating that their conformation is dominated instead by the steric bulk of the Cp* group. Close contacts between Fe atoms and Cp rings to which the metal is not directly bound have been distinguished in the crystal structures of trimetallic $[Fe(FcEMe_2C_5H_4)_2]$ ($E = C$,[27] Si[28]) and pentametallic $[Fe(FcSiMe_2fcSiMe_2C_5H_4)_2]$ ($fc = 1,1'$-ferrocenediyl[29]); for these both intra- and intermolecular contacts are seen and the molecules stack in layers with their arrangement determined by non-bonded Fe–Cp electrostatic interactions, the magnitude of which presumably surpasses any unfavourable intramolecular conformations. The packings of **CoA**, **CoB** and **FeC** show similar motifs, although with these bimetallics only *inter*molecular close contact is possible; this causes the molecules to arrange themselves in chains, giving a herringbone-like pattern in one plane which is stacked perpendicular to this (see Figure 1c for packing in the **CoB** structure).

Magnetic data: The magnetic properties of **CoA–CoC** in the solid state from 5–350 K were investigated by variable-temperature SQUID magnetometry. The data are presented below in Figure 2 as a plot of μ_{eff} ($= \sqrt{(8\chi_m T)}$) versus T (see Supporting Information for a plot of χ_m vs T). The molar susceptibility data for **CoA** were fitted to the Curie–Weiss law; the derived magnetic moment varies little with temperature above 20 K and is close to that expected for two independent $S = \frac{1}{2}$ Co centres at 300 K (2.45 μ_B). The molar susceptibilities of **CoB** and **CoC** show significant deviations from Curie–Weiss behaviour, indicative of spin–spin exchange interactions; the respective magnetic moments are
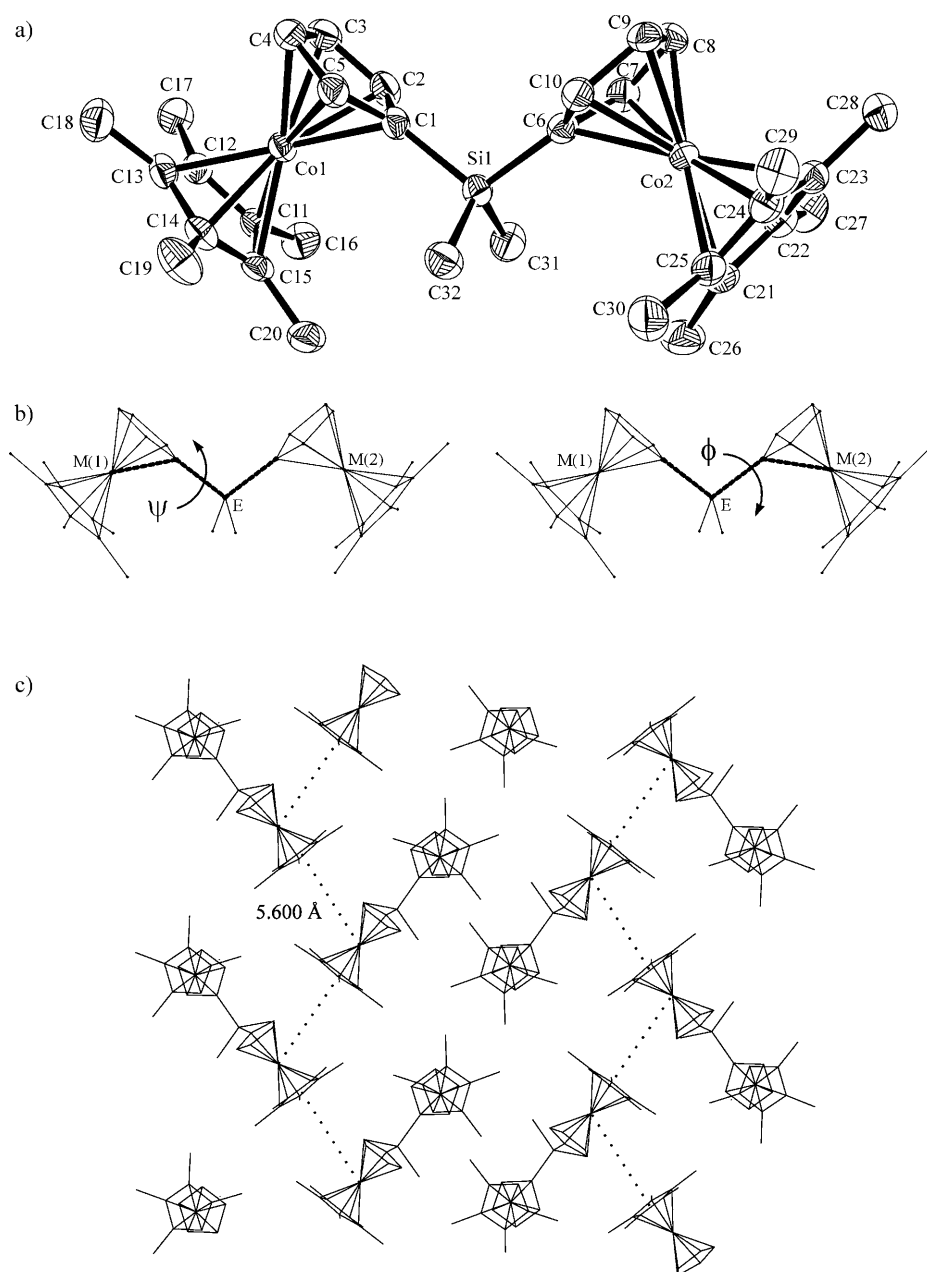
Scheme 1. Synthesis of **FeA–FeD** and **CoA–CoC**.

FeA X = CMe₂   CoA X = CMe₂
FeB X = SiMe₂   CoB X = SiMe₂
FeC X = GeMe₂   CoC X = GeMe₂
FeD X = Si(Me)₂Si(Me)₂

Figure 1. a) Structure of **CoB**; b) definitions of torsion angles ψ and φ; c) projection of the bc plane in the **CoB** structure showing intermolecular close contact between Co1 and the adjacent Cp ring, forming chains.

smaller than found for **CoA** at 300 K and decrease rapidly with decreasing temperature. The susceptibilities of **CoB** and **CoC** were fit to the Bleaney–Bowers equation [Eq. (1)] describing antiferromagnetic coupling between two $S=\frac{1}{2}$ centres to give an $S=0$ ground state and an $S=1$ excited state

$$\chi_m = \left(\frac{2 N_A g^2 \mu_B^2}{3k(T-\theta)} \right) \left(\frac{1}{1 + (1/3)e^{-2J/kT}} \right) \qquad (1)$$

The parameters obtained from the least-squares fits are collected in Table 1; the g values observed are reduced

slightly from the free-electron value, consistent with what is found by EPR and magnetic susceptibility for mononuclear cobaltocenes.[9,30,31] The antiferromagnetic coupling, J, between Co centres is slightly greater through $SiMe_2$ than through $GeMe_2$; any magnetic coupling in the CMe_2-bridged species is presumably too weak to be detected experimentally. The near-isostructural nature of **CoA** and **CoB** suggests that the dominant effect is *intra*molecular in nature, involving through-bond coupling (which is expected to be greater through $SiMe_2$ than through CMe_2). The magnitude of antiferromagnetic coupling in both **CoB** and **CoC** is small, somewhat weaker than found for bimetallic cobaltocenes and their analogues connected in a *para*-arrangement by a benzene ring,[32,33] and significantly smaller than for $[Co_2Fv_2]$ and dicobaltbis(pentalene), which are both diamagnetic.[34,35]

Electrochemistry: **FeA–FeD** and **CoA–CoC** all display reversible, overlapping oxidations to the M^{III}–M^{II} and M^{III}–M^{III} mono- and dications by cyclic voltametry (CV) in THF/0.1 M nBu_4PF_6; the Co species also show reversible, overlapping reductions to the Co^{II}–Co^I and Co^I–Co^I mono- and dianions (Figure 3). The data are summarised in Table 2. The peak-to-peak separation between individual oxidations/reductions (ΔE) is small, consistent with limited interaction between the metal centres. Better resolution of successive oxidation events was obtained for the ferrocenes by square-wave voltammetry; unfortunately, this experiment was unsuccessful for the cobaltocenes, possibly due to adsorption of ionic species onto the electrode.[36] Accurate ΔE values from square-wave voltammetry for the ferrocenes show the electrochemical separation between redox waves decreases for the bridging ligand in the order $CMe_2 > SiMe_2 > GeMe_2$, consistent with increasing metal separation and a through-space, essentially electrostatic effect; these values are of similar magnitude to those found for other species linked by saturated
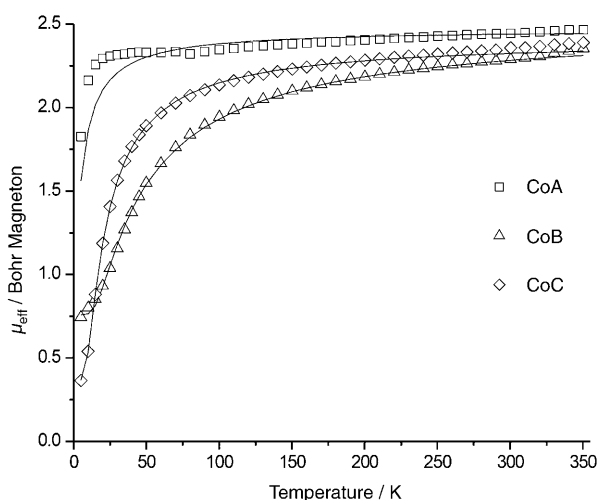
Figure 2. Change in effective magnetic moment with temperature for **CoA–CoC**. Here $\mu_{eff} = \sqrt{(8\chi_m T)}$; χ_m was measured by variable-temperature SQUID magnetometry. The markers depict the experimental data, while the solid lines are derived from theoretical fits using the parameters in Table 1.

Table 1. Parameters derived from least-squares fitting of the variable-temperature magnetic susceptibility data to the Curie–Weiss law (**CoA**) or Bleaney–Bowers equation (**CoB** and **CoC**).

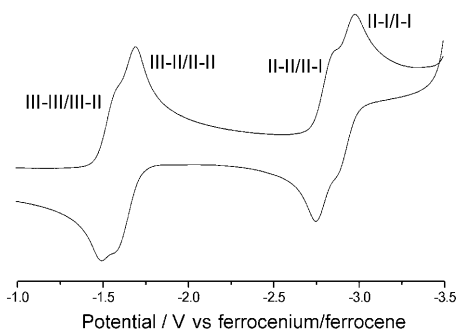|	g	θ [K]	J [cm^{-1}]	μ_{eff} (300 K) [μ_B]
CoA	1.75	−8	n/a	2.44
CoB	1.95	−50	−21	2.29
CoC	1.95	−13	−14	2.36

Figure 3. Cyclic voltammogram of **CoA** in THF/0.1 M nBu$_4$NPF$_6$ showing the four metallocene redox couples.

bridges. Direct comparison is possible between **FeA** and diferrocenylmethane [Fc$_2$CH$_2$], for which differential pulse voltammetry in MeCN reveals ΔE values of 0.17 and 0.13 V,[37] respectively, for the two complexes; the larger ΔE for **FeA** may reflect a difference in solvation effects upon methylation of the bridge and Cp rings. Although ΔE tends to be much greater when the complex has significant through-bond metal–metal coupling in addition to an electrostatic interaction, for example, in biferrocene [{Fe(Cp)}$_2$-

Table 2. Half-wave potentials for **FeA–FeD** and **CoA–CoC** in THF/0.1 M nBu$_4$PF$_6$; all values are in V. Separations between peaks for the one-electron oxidations of **FeD** and the one-electron reductions of **CoB** and **CoC** were not resolvable by CV. ΔE values quoted for the Fe species were measured by square-wave voltammetry.

	$E_{1/2}$ (III-III/III-II)	$E_{1/2}$ (III-II/II-II)	ΔE	$E_{1/2}$ (II-II/II-I)	$E_{1/2}$ (II-I/I-I)
FeA	−0.21	−0.35	0.113	–	–
FeB	−0.18	−0.25	0.093	–	–
FeC	−0.20	−0.26	0.074	–	–
FeD		−0.25	0	–	–
CoA	−1.54	−1.64	–	−2.80	−2.93
CoB	−1.49	−1.60	–	−2.78	
CoC	−1.51	−1.61	–	−2.80	

(μ-Fv)] ($\Delta E = 0.33$ V in MeCN) and in bis(fulvalene)diiron (0.59 V in MeCN),[37] it is often a poor quantitative measure of electronic coupling and has been shown to be extremely medium-dependent.[38] Electronic coupling can be probed more quantitatively using Hush theory, as described in the next section.

Electronic spectroscopy of the mixed-valence monocationic species: **FeA–FeD** and **CoA–CoC** were oxidised by reaction with [Fe(Cp)$_2$]$^+$[BAr$'_4$]$^-$ in THF to form the MV monocations that were investigated by UV-visible-NIR spectroscopy. Use of [BAr$'_4$]$^-$ (BAr$'_4$=3,5-((CF$_3$)$_2$C$_6$H$_3$)$_4$B) as the counterion proved advantageous as the mono- and dicationic dinuclear metallocene species generated remained soluble and calculation of the concentration of monocation and, hence, absorptivity of the IVCT band was not affected by precipitation of unknown quantities of material; moreover the side-product, ferrocene, does not interfere in the spectral region of interest. Quantitative analysis of the spectra required correction of the absorption values observed for the concentration of the MV species present. The small ΔE values observed between successive oxidations indicate low values of the comproportionation constant (K_c) for the equilibrium given in Equation (2) ($K_c \leq 80$) and, hence, significant disproportionation occurs upon addition of one equivalent of oxidising agent to neutral material.

$$[\text{neutral}] + [\text{dication}]^{2+} \rightleftharpoons 2[\text{monocation}]^+ \quad (2)$$
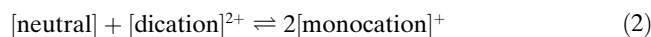
The concentration of the monocationic species at equilibrium was determined from the physically reasonable solution to the quadratic equation [Eq. (3)], in which [M$^+$] is the concentration of monocation at equilibrium, C_M is the concentration of M in reaction mixture (i.e., neutral, monocation and dication), C_{OX} is the concentration of [Fe(Cp)$_2$]$^+$[BAr$'_4$]$^-$ in reaction mixture and K_c is the comproportionation constant.

$$(0.25-(1/K_c))[\text{M}^+]^2-(0.5\,C_M)[\text{M}^+] + (0.25\,C_{OX})(2\,C_M-C_{OX}) = 0 \quad (3)$$

Accurate K_c values were obtainable for the Fe systems only, by using ΔE from square-wave experiments (vide supra). For the Co systems the K_c value for the corresponding Fe compound was used; this is reasonable as K_c is likely to be dominated by electrostatic factors and the geometries of the Fe and Co complexes are very similar. However, this may lead to an underestimation of $[M^+]$ as the K_c values are likely to be slightly larger for Co (due to the greater electronic coupling in the Co species) and hence ε_{max} for the IVCT band may be overestimated; consequences of this are considered below. For **FeD** no peak separation was resolvable and the entropic value ($K_c = 4$)[39, 40] was used; as above this is likely to be an underestimate (at least some electrostatic stabilisation is expected) and hence will result in an overestimate for ε_{max}.

The lowest energy band observed in the spectrum occurs in the NIR region in all cases; this band is assigned to the IVCT transition in the monocation and was assumed to be exclusively due to this species, allowing calculation of the absorption coefficient. NIR spectra for the Fe species are shown in Figure 4; the higher-energy band observed for these Fe species peaks around $13\,500$ cm^{-1} and is presumably due to Cp-to-Fe^{III} charge-transfer transitions in the ferrocenium units of the mono- and dications.[41]

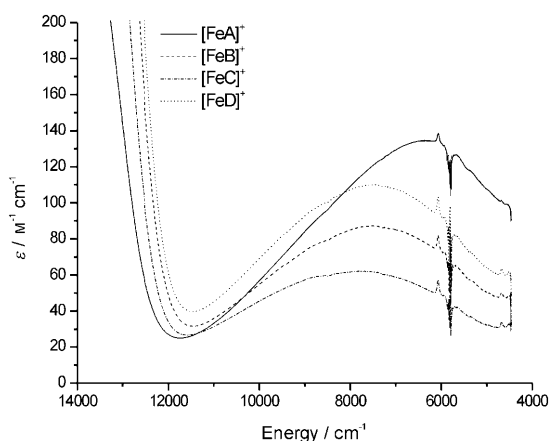
Figure 4. NIR spectra of **FeA–FeD** in THF after addition of ca. 1 equiv $[FeCp_2]^+[BAr'_4]^-$, showing the low-energy IVCT transition of the monocations.

The IVCT band has significantly lower intensity for the Fe species than for Co, as depicted for $[\mathbf{FeB}]^+$ and $[\mathbf{CoB}]^+$ in Figure 5. In all cases, this low-energy band is approximately symmetrical and is broader than the Hush limit for Class II MV species ($\Delta\tilde{\nu}_{1/2} = \sqrt{(2310\,\tilde{\nu}_{max})}$),[1] as expected for a weak electronic coupling situation arising from the mixing of donor and acceptor units through a saturated bridge. The electronic coupling parameter, V, and the delocalisation coefficient, α, in the ground-state wavefunction (φ) were extracted by analysis of the IVCT band using Hush's relationships [Eqs. (4) and (5)].[1]
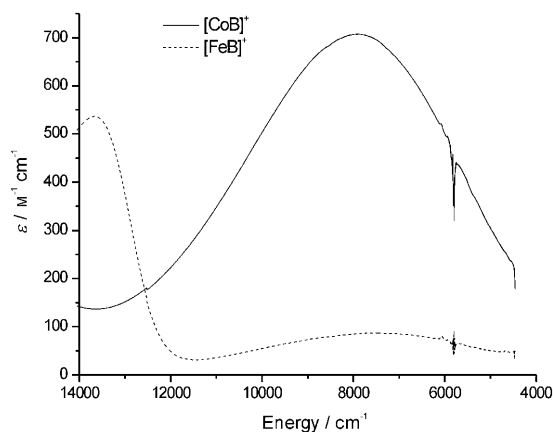

Figure 5. NIR spectra of **FeB** and **CoB** in THF after addition of approximately one equivalent of $[FeCp_2]^+[BAr'_4]^-$, showing the relative intensities of the low-energy IVCT transition in the monocations; the y axis scale is valid only for this band.

$$V = 2.05 \times 10^{-2}(\varepsilon_{max}\,\tilde{\nu}_{max}\,\Delta\tilde{\nu}_{1/2})^{1/2}/r \qquad (4)$$

$$\alpha = V/\tilde{\nu}_{max} \qquad (5)$$

$$\varphi = \sqrt{(1-\alpha^2)}\psi_A + \alpha\psi_B$$

The distance between donor and acceptor units, r, is unknown, as the complexes are expected to be conformationally flexible in solution. However, a molecular mechanics study of CMe$_2$- and SiMe$_2$-bridged ferrocene systems shows that the metal–metal distance must fall within the range 4.5–7.5 Å;[26] these values were used in the calculations to give a range of possible values for V for the CMe$_2$-, SiMe$_2$- and GeMe$_2$-bridged complexes. Corresponding values for Si$_2$Me$_4$-bridged **FeD** were not calculated, as there is presumably a much wider range of conformations possible. Table 3 provides a summary of the band energies, bandwidths and the calculated ranges of V and α for the monocations.

Several points arise from the data presented in Table 3. Firstly, $\tilde{\nu}_{max}$ for a given Co species is greater than for the analogous Fe complex. In a Class II system the IVCT band energy represents the reorganisation energy, λ, for the intramolecular electron-transfer reaction. This implies larger reorganisation energy for each respective Co species, which is consistent with the somewhat antibonding character of the cobaltocenium/cobaltocene LUMO/HOMO. Estimations from vibrational data[3] suggest that the difference in internal reorganisation energy between the cobaltocenium/cobaltocene and ferrocenium/ferrocene couples is of the order of 100 cm^{-1}. The differences in $\tilde{\nu}_{max}$ observed for the dinuclear metallocenes above are somewhat larger that twice this value (900–230 cm^{-1}), which may reflect conformational effects (amongst others) contributing to dissimilar *external* reorganisation energies for Fe and Co species. The value of $\tilde{\nu}_{max}$ increases slightly with the size of the bridging atom, presumably due to differences in external reorganisation energy; as the metal–metal separation increases the electron transfer distance will increase and hence the solvent reorganisation parameter becomes larger.

Table 3. IVCT band data for the monocations of **FeA**–**FeD** and **CoA**–**CoC** in THF; missing values were not calculated as discussed in the text.

	$\tilde{\nu}_{max}$ [cm^{-1}]	ε_{max} [M^{-1}cm^{-1}]	$\Delta\tilde{\nu}_{1/2}$ (obsd) [cm^{-1}]	$\Delta\tilde{\nu}_{1/2}$ (Hush) [cm^{-1}]	V [cm^{-1}]	α
[FeA]$^+$	6350	134	6000	3830	202–337	0.032–0.053
[FeB]$^+$	7480	87	6130	4160	179–298	0.024–0.039
[FeC]$^+$	7750	62	6120	4230	153–256	0.019–0.033
[FeD]$^+$	7500	110	5920	4160	–	–
[CoA]$^+$	7250	1433	5230	4090	659–1098	0.090–0.152
[CoB]$^+$	7900	707	5680	4270	504–840	0.064–0.106
[CoC]$^+$	7980	223	6370	4290	301–502	0.037–0.063

The values of V and α are significantly larger for the cobaltocene systems than for the ferrocene systems, presumably due to the orbitals involved having greater delocalization onto the ligand and hence greater donor–acceptor overlap possible in the Co case. Note that even the smallest value in the range calculated for a given Co species is greater than the largest value for the corresponding Fe complex, and hence the difference observed between Fe and Co cannot be accounted for by dissimilar conformational preferences in the two systems. The values calculated for Co may, however, be overestimated due to use of K_c for the Fe system, which will overestimate ε_{max} for the IVCT band and hence increase the calculated value of V for Co. The maximum value of this error (calculated assuming [M$^+$]=concentration of [Fe(Cp)$_2$]$^+$[BAr'$_4$]$^-$ in the reaction mixture) reduces the values to approximately 80% of their reported magnitude; thus, V and α are still substantially greater for the Co systems after taking this into account.

The degree of electronic coupling decreases in the order CMe$_2$ > SiMe$_2$ > GeMe$_2$ for both Fe and Co systems. This observation is unusual in light of previous results on metallocenes linked by saturated bridges. Electronic coupling between ferrocenyl groups linked by a saturated carbon bridge has been observed only for the very weakly coupled triferrocenylmethane ion, [Fc$_3$CH]$^+$ (V=24 cm^{-1}, α=0.004)[16] and the zwitterionic ferricenyl(III)tris(ferrocenyl(II))borate [Fc$_4$B] ($\tilde{\nu}_{max}$=4550 cm^{-1} in CH$_2$Cl$_2$, although no analysis of this band is given).[42] In both cases the IVCT transition in these highly crowded species is thought to occur by means of a through-space mechanism. Previous attempts to measure an IVCT band for analogous [Fc$_2$CH$_2$]$^+$ and [Fc$_3$B]$^+$ ions were unsuccessful,[16] although here we show CMe$_2$-bridged [FeA]$^+$ to display an IVCT band of considerable intensity. On the other hand, the values of V and α obtained for [FeB]$^+$ (179–278, 0.024–0.039) are similar (although slightly larger) to those previously reported for [Fc$_2$SiMe$_2$]$^+$ (V=169 cm^{-1}, α=0.02; here the electron transfer distance was taken to be 5.82 Å).[41] Previous authors have proposed stronger coupling to be seen through a Si-bridge,[2,43,44] although most studies have depended upon electrochemical data and have not compared direct CR$_2$- and SiR$_2$-bridged analogues under identical conditions. It has been suggested that conjugation[45] through empty, low-lying σ*- or d-orbitals of Si may facilitate greater coupling in this case.[46]

Here, however, where we have direct CMe$_2$ and SiMe$_2$ analogues, we find stronger coupling with a carbon bridge.[47] Moreover, we have directly measured electronic coupling in the MV species rather than relying on ΔE data (which are determined by more factors than just V). Presumably, then, the decrease in the order CMe$_2$ > SiMe$_2$ > GeMe$_2$ indicates that the coupling is largely through space in these species. Moreover, assuming the same molecular conformation, the metal–metal separation should increase with the size of the bridging atom; the distance parameter, r, consequently should increase and hence the calculated values for V and α in the SiMe$_2$ and GeMe$_2$ systems may be overestimated, reinforcing the observed trend. The observation of strong IVCT in [FeD]$^+$ underlines the importance of strong through-space effects.

The unexpectedly-large coupling observed for [FeA]$^+$ in THF prompted us to study this complex further. The lowest energy transition for [FeA]$^+$ displays significant solvatochromism, confirming the charge-transfer origin of this band; use of [BAr'$_4$]$^-$ as the counterion enabled investigation of this solvatochromism across a wide range of solvent polarity, allowing generation of soluble cationic species even in Et$_2$O and toluene. Hush theory relates the energy of a Class II IVCT band to the inner- and outer-sphere reorganisation energies, λ_i and λ_o respectively, [Eq. (6)].[1]

$$\tilde{\nu}_{max} = \lambda_i + \lambda_o \tag{6}$$

The outer-sphere reorganisation energy may be analysed in terms of a dielectric continuum model for the solvent, which for a single electron transfer event may be written as Equation (7),[48] in which a_1 and a_2 are the molecular radii of the redox centers, d is the electron-transfer distance, and n and D are the solvent refractive index and dielectric constant respectively.

$$\lambda_o = e^2(1/a_1 + 1/a_2 - 1/d)(1/n^2 - 1/D) \tag{7}$$

Figure 6 shows the values of $\tilde{\nu}_{max}$ plotted against $(1/n^2 - 1/D)$, confirming the expected linear relationship. Interestingly, the IVCT band shows a greater red-shift in CH$_2$Cl$_2$ than expected; this has been observed for a variety of charge-transfer bands in other metallocene systems and may be due to a specific interaction between the metallocene unit and this solvent.[15,49,50] A least-squares linear fit of the solvatochromic data gives the y intercept (λ_i) at 3587 cm^{-1}; this value is very similar to the internal reorganisation energy found for biferrocene (3500 cm^{-1}) in a comparable study.[51] The electron-transfer distance (d) may be estimated from the slope of the line; depending on the values chosen for a_1 and a_2[52] this falls in the range 5.08–7.44 Å, completely con-
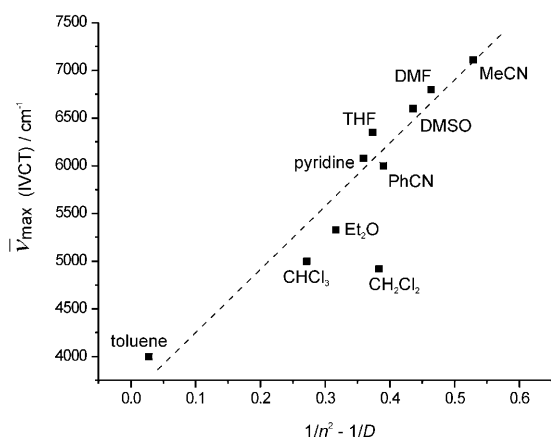
Figure 6. Solvatochromism of the lowest energy transition for [**FeA**]$^+$.

sistent with the range of values for metal–metal distance obtained from molecular mechanics used above as estimates for the diabatic electron-transfer distance in the calculations.

Conclusion

These results show that through-space electronic coupling can be important in metallocene systems connected by saturated bridges, with significant values of V and α possible in both Fe and Co systems. For the first time in a directly comparable series of compounds, it has been observed that the order of V and α values for a given metal changes with the bridging atom in the order $CMe_2 > SiMe_2 > GeMe_2$. This suggests that a through-space mechanism is operative in all cases and, hence, that through-bond coupling is relatively unimportant; IVCT for the CMe_2-bridged systems must be purely through-space as no appropriate orbitals are available on the carbon atom for through-bond mixing. This is in contrast to previous speculation that delocalisation should be greater through a saturated Si-based bridge than through its C-bridged analogue. In all cases, the electronic coupling is notably greater for the linked Co metallocenes; [**CoA**]$^+$ and [**CoB**]$^+$ exhibit appreciable delocalisation similar to the biferrocene cation ($\alpha = 0.09$). This suggests that cobaltocene-based materials might well possess more interesting electronic properties than their Fe analogues, such as the poly-(ferrocenylsilanes) which have been well-studied.[53] To date, syntheses of cobaltocene-based polymers remain elusive; although a two-carbon-bridged cobaltocenophane has been reported attempts to polymerise this species have proven unsuccessful.[54] Suitable precursors to polymeric cobaltocene materials therefore represent interesting targets for future synthetic efforts.

Experimental Section

All reactions were performed under an inert atmosphere of dinitrogen utilising standard Schlenk techniques or in a Vacuum Atmospheres glovebox. Solvents were dried by reflux over the appropriate drying agent, distilled under a flowing stream of dinitrogen and stored in flame-dried ampoules. These were thoroughly degassed before use by passage of a stream of dinitrogen through the solvent. The following compounds were prepared according to published procedures: [Fe(Cp*)Cl(tmeda)],[17] [Co(Cp*)Cl]$_2$,[55] [Li$_2$(C$_5$H$_4$)$_2$CMe$_2$],[56,57] [Li$_2$(C$_5$H$_4$)$_2$SiMe$_2$],[57,58] [Li$_2$-(C$_5$H$_4$)$_2$GeMe$_2$],[57,59] [Li$_2${(C$_5$H$_4$)Si(Me)$_2$}$_2$],[57,60] [Fe(Cp)$_2$]$^+$[BAr′$_4$]$^-$.[61]

Synthesis of FeA–FeD: The synthesis of **FeA** is described: a suspension of [Li$_2$(C$_5$H$_4$)$_2$CMe$_2$] (0.13 g, 0.73 mmol) in THF (30 mL) was added to a stirred solution of [Fe(Cp*)Cl(tmeda)] (0.50 g, 1.46 mmol) in THF (30 mL). The resulting orange solution was stirred overnight; volatiles were then removed in vacuo and the residue extracted with Et$_2$O (3 × 30 mL) and filtered through Celite. Concentration of the filtrate (ca. 20 mL) and cooling to −35 °C afforded **FeA** as orange, air-stable crystals. Syntheses of **FeB–FeD** are analogous and were achieved by substituting for [Li$_2$(C$_5$H$_4$)$_2$CMe$_2$] the respective lithium salt of the ligand (0.5 equivalents to [Fe(Cp*)Cl(tmeda)]) in the preparation described for **FeA**.

Data for FeA: Yield: 0.25 g, 0.45 mmol, 62 %; ^{1}H NMR (300 MHz, C$_6$D$_6$, 300 K): $\delta = 3.54$ (s, 4H), 3.42 (s, 4H), 1.85 (s, 30H), 1.75 ppm (s, 6H); ^{13}C {^{1}H} NMR (75 MHz, C$_6$D$_6$, 300 K): $\delta = 103.1$ (*C* quat), 79.4 (*C* quat), 72.0 (*C*H), 67.4 (*C*H), 33.6 (*C* quat.), 28.5 (*C*H$_3$), 11.9 ppm (*C*H$_3$); MS (EI): m/z (%): 552 (13) [*M*]$^+$; elemental analysis calcd (%) for C$_{33}$H$_{44}$Fe$_2$ (552.40): C 71.75, H 8.03; found: C 71.67, H 8.08.

Data for FeB: Yield: 0.23 g, 0.40 mmol, 55 %; ^{1}H NMR (300 MHz, C$_6$D$_6$, 300 K): $\delta = 3.73$ (s, 4H), 3.67 (s, 4H), 1.83 (s, 30H), 0.64 ppm (s, 6H); ^{13}C {^{1}H} NMR (75 MHz, C$_6$D$_6$, 300 K): $\delta = 79.7$ (*C* quat), 75.4 (*C*H), 75.3 (*C*H), 73.9 (*C* quat.), 11.9 (*C*H$_3$), −0.7 ppm (*C*H$_3$); MS (EI): m/z (%): 568 (12) [*M*]$^+$; elemental analysis calcd (%) for C$_{32}$H$_{44}$Fe$_2$Si (568.48): C 67.61, H 7.80; found: C 67.55, H 7.87.

Data for FeC: Yield: 0.23 g, 0.38 mmol, 52 %; ^{1}H NMR (300 MHz, C$_6$D$_6$, 300 K): $\delta = 3.74$ (s, 4H), 3.64 (s, 4H), 1.84 (s, 30H), 0.73 ppm (s, 6H); ^{13}C {^{1}H} NMR (75 MHz, C$_6$D$_6$, 300 K): δ 79.7 (*C* quat), 76.7 (*C* quat), 74.7 (*C*H), 74.6 (*C*H), 11.9 (*C*H$_3$), −0.9 ppm (*C*H$_3$); MS (EI): m/z (%): 614 (80) [*M*]$^+$; elemental analysis calcd (%) for C$_{32}$H$_{44}$Fe$_2$Ge (612.98): C 62.70, H 7.23; found: C 62.41, H 7.62.

Data for FeD: Yield: 0.19 g, 0.30 mmol, 41 %; ^{1}H NMR (300 MHz, C$_6$D$_6$, 300 K): $\delta = 3.78$ (s, 4H), 3.48 (s, 4H), 1.80 (s, 30H), 0.37 ppm (s, 12H); ^{13}C {^{1}H} NMR (75 MHz, C$_6$D$_6$, 300 K): δ 79.8 (*C* quat), 75.3 (*C*H), 75.2 (*C*H), 72.3 (*C* quat), 12.0 (*C*H$_3$), −4.2 ppm (*C*H$_3$); MS (EI): m/z (%): 626 (52) [*M*]$^+$; elemental analysis calcd (%) for C$_{34}$H$_{50}$Fe$_2$Si$_2$ (626.63): C 65.17, H 8.04; found: C 65.32, H 8.46.

Synthesis of CoA–CoC: The synthesis of **CoA** is described: a suspension of [Li$_2$(C$_5$H$_4$)$_2$CMe$_2$] (0.34 g, 1.83 mmol) in THF (30 mL) was added to a stirred solution of [{Co(Cp*)Cl}$_2$] (0.84 g, 1.83 mmol) in THF (30 mL). The resulting green solution was stirred overnight; volatiles were then removed in vacuo and the residue extracted with Et$_2$O (3 × 30 mL) and filtered through Celite. Concentration of the filtrate (ca. 20 mL) and cooling to −35 °C afforded **CoA** as dark green, air-sensitive crystals. Syntheses of **CoB** and **CoC** are analogous and were achieved by substituting for [Li$_2$(C$_5$H$_4$)$_2$CMe$_2$] the respective lithium salt of the ligand (1 equiv to [{Co(Cp*)Cl}$_2$]) in the preparation descibed for **CoA**.

Data for CoA: Yield: 0.40 g, 0.72 mmol, 40 %; ^{1}H NMR (500 MHz, C$_6$D$_6$, 300 K): $\delta = 38.77$ (s, 30H), 4.98 (s, 6H), −43.34 (br, 4H), −55.84 ppm (br, 4H); IR (KBr): $\tilde{\nu} = 2968$ (s), 2906 (s), 2854 (s), 1614 (w), 1466 (m), 1448 (m), 1378 (s), 1356 (m), 1024 (s), 778 cm^{-1} (s); MS (EI): m/z (%): 558 (100) [*M*]$^+$; elemental analysis calcd (%) for C$_{33}$H$_{44}$Co$_2$ (558.58): C 70.96, H 7.94; found: C 70.30, H 8.09.

Data for CoB: Yield: 0.45 g, 0.78 mmol, 44 %; ^{1}H NMR (500 MHz, C$_6$D$_6$, 300 K): $\delta = 37.77$ (s, 30H), 7.82 (s, 6H), −7.46 (br, 4H), −53.87 ppm (br, 4H); IR (KBr): $\tilde{\nu} = 2970$ (s), 2904 (s), 2856 (s), 1608 (w), 1420 (m), 1378 (s), 1352 (m), 1242 (s), 1160 (s), 1030 (s), 804 (s), 782 cm^{-1} (s); MS (EI): m/z (%): 574 (95) [*M*]$^+$; elemental analysis calcd (%) for C$_{32}$H$_{44}$Co$_2$Si (574.65): C 66.88, H 7.72; found: C 66.57, H 7.69.

Data for CoC: Yield: 0.28 g, 0.45 mmol, 46%; ^1H NMR (300 MHz, C$_6$D$_6$, 300 K): $\delta = 37.83$ (s, 30H), 4.32 (s, 6H), −16.72 (br, 4H), −54.95 ppm (br, 4H); IR (KBr): $\tilde{v} = 2964$ (s), 2906(s), 2854 (s), 1618 (w), 1420 (m), 1378 (s), 1232 (s), 1150 (s), 1024 (s), 800 (s), 780 cm^{-1} (s); MS (EI): m/z (%): 620 (88) [M]$^+$; elemental analysis calcd (%) for C$_{32}$H$_{44}$Co$_2$Ge (619.16): C 62.08, H 7.16; found: C 62.27, H 7.29.

Physical measurements: Solid-state magnetic susceptibility data were obtained using a Quantum Design MPMS-5 SQUID magnetometer. Accurately weighed powdered samples of about 0.05 g were loaded into gelatine capsules in a glove-box and placed between additional gelatine capsules in a non-magnetic plastic straw, which was then lowered into the cryostat. The sample was therefore mounted in a weakly diamagnetic medium and no correction was made for the diamagnetism of the sample-holder. The field independence of the susceptibility data was verified by measuring the susceptibility as a function of field between −5 and +5 T. Data were then measured employing fields of 0.1 and 0.5 T and were corrected for the inherent diamagnetism of the sample by use of Pascal's constants;[62] these diamagnetic corrections had values of 355.72×10^{-6}, 369.72×10^{-6} and 374.72×10^{-6} cm^3 mol^{-1} for **CoA**, **CoB** and **CoC**, respectively. Additionally, the fits for **CoB** and **CoC** included a correction for a small amount of Curie impurity evident from low-temperature data.

Electrochemical measurements were performed at room temperature by using a BAS potentiostat with a glassy-carbon working electrode supported by platinum wire auxiliary and AgCl/Ag pseudo-reference electrodes. Measurements were made on deoxygenated solutions approximately 5×10^{-4} M in sample and 0.1 M in [nBu$_4$N]$^+$[PF$_6$]$^-$ as supporting electrolyte. Solvents (THF, MeCN) were freshly distilled before use. Measurements on air-sensitive samples **CoA–CoC** were made under a N$_2$ atmosphere in a specially constructed cell with a sidearm fitted with a Rotaflo tap; solutions of the sample and supporting electrolyte were transferred through a cannula into the cell. Potentials were referenced to the ferrocenium/ferrocene couple at 0.00 V by addition of [Fe(Cp)$_2$] to the cell. The reversibility of the redox couple was judged by comparison with the behaviour of the ferrocenium/ferocene couple under the same conditions. Experimental parameters used: CV scan rate 50 mV s^{-1}; SWV scan rate 10 mV s^{-1}, pulse amplitude = 50 mV, step height 6 mV, pulse period 20 ms; DPV scan rate 10 mV s^{-1}, sample width = 17 ms, pulse amplitude = 40 mV, pulse width = 50 ms, pulse period = 200 ms.

Oxidised species were generated in situ by adding an accurately measured amount of [Fe(Cp)$_2$]$^+$[BAr$'_4$]$^-$ in THF (approximately one equivalent) by syringe to a dry solution of the respective compound in THF under N$_2$. The solution was diluted by using syringes to an appropriate concentration for electronic spectroscopy, transferred to an airtight 1 cm cell and immediately investigated by UV-visible-NIR spectroscopy. UV-visible-NIR spectra were recorded on a Varian Cary 5 spectrometer (range 190–3300 nm). The NIR band was analysed by correcting for the concentration of the MV monocation present, as described in the text.

CCDC-263600, CCDC-263601 and CCDC-263602 contain the supplementary crystallographic data for this paper. These data can be obtained free of charge from the Cambridge Crystallographic Data Centre via www.ccdc.cam.ac.uk/data_request/cif.

Acknowledgements

[1] N. S. Hush, *Prog. Inorg. Chem.* **1967**, *8*, 391.
[2] S. Barlow, D. O'Hare, *Chem. Rev.* **1997**, *97*, 637.
[3] R. M. Nielson, M. N. Golovin, G. E. McManis, M. J. Weaver, *J. Am. Chem. Soc.* **1988**, *110*, 1745.
[4] R. M. Nielson, G. E. McManis, M. N. Golovin, M. J. Weaver, *J. Phys. Chem.* **1988**, *92*, 3441.
[5] G. E. McManis, R. M. Nielson, A. Gochev, M. J. Weaver, *J. Am. Chem. Soc.* **1989**, *111*, 5533.
[6] D. K. Phelps, J. R. Gord, B. S. Freiser, M. J. Weaver, *J. Phys. Chem.* **1991**, *95*, 4338.
[7] M. C. Zerner, G. H. Loew, R. F. Kirchner, U. T. Mueller-Westerhoff, *J. Am. Chem. Soc.* **1980**, *102*, 589.
[8] J. Weber, A. Goursot, E. Penigault, J. H. Ammeter, J. Bachmann, *J. Am. Chem. Soc.* **1982**, *104*, 1491.
[9] J. H. Ammeter, J. D. Swalen, *J. Chem. Phys.* **1972**, *57*, 678.
[10] M. B. Robin, P. Day, *Adv. Inorg. Chem. Radiochem.* **1967**, *10*, 247.
[11] G. E. McMannis, R. M. Nielson, M. J. Weaver, *Inorg. Chem.* **1988**, *27*, 1827.
[12] J. M. Manriquez, M. D. Ward, W. M. Reiff, J. C. Calabrese, N. L. Jones, P. J. Carroll, E. E. Bunel, J. S. Miller, *J. Am. Chem. Soc.* **1995**, *117*, 6182.
[13] M.-H. Delville, S. Rittinger, D. Astruc, *J. Chem. Soc. Chem. Commun.* **1992**, 519.
[14] M.-H. Delville, F. Robert, P. Gouzerh, J. Linares, K. Boukheddaden, F. Varret, D. Astruc, *J. Organomet. Chem.* **1993**, *451*, C10.
[15] S. Barlow, *Inorg. Chem.* **2001**, *40*, 7047.
[16] F. Delgado-Pena, D. R. Talham, D. O. Cowan, *J. Organomet. Chem.* **1983**, *253*, C43.
[17] K. Jonas, P. Klusmann, R. Goddard, *Z. Naturforsch. B* **1995**, *50*, 394.
[18] O. M. Heigl, M. A. Herker, W. Hiller, F. H. Köhler, A. Schell, *J. Organomet. Chem.* **1999**, *574*, 94.
[19] Y. Ohki, H. Suzuki, *Angew. Chem.* **2000**, *112*, 3250; *Angew. Chem. Int. Ed.* **2000**, *39*, 3120.
[20] J. M. Manriquez, E. E. Bunel, B. Oelckers, *Inorg. Synth.* **1997**, *31*, 214.
[21] J. R. Morrow, D. Astruc, *Bull. Soc. Chim. Fr.* **1992**, *129*, 319.
[22] F. Köhler, *J. Organomet. Chem.* **1976**, *110*, 235.
[23] H. Wadepohl, C.-W. von der Lieth, F.-J. Paffen, H. Pritzkow, *Chem. Ber.* **1995**, *128*, 317.
[24] P. Hudeczek, F. Köhler, P. Bergerat, O. Kahn, *Chem. Eur. J.* **1999**, *5*, 70.
[25] S. Barlow, A. L. Rohl, D. O'Hare, *Chem. Commun.* **1996**, 257.
[26] S. Barlow, A. L. Rohl, S. Shi, C. J. Freeman, D. O'Hare, *J. Am. Chem. Soc.* **1996**, *118*, 7578.
[27] S. Barlow, V. J. Murphy, J. S. O. Evans, D. O'Hare, *Organometallics* **1995**, *14*, 3461.
[28] K. H. Pannell, V. V. Dementiev, H. Li, F. Cervantes-Lee, M. T. Nguyen, A. F. Diaz, *Organometallics* **1994**, *13*, 3644.
[29] R. Rulkens, A. J. Lough, I. Manners, *J. Am. Chem. Soc.* **1994**, *116*, 797.
[30] E. König, R. Schnakig, S. Kremer, B. Kanellakopulos, R. Klenze, *Chem. Phys.* **1978**, *27*, 331.
[31] J. L. Robbins, N. Edelstein, B. Spencer, J. C. Smart, *J. Am. Chem. Soc.* **1982**, *104*, 1882.
[32] J. M. Manriquez, M. D. Ward, J. C. Calabrese, P. J. Fagan, A. J. Epstein, J. S. Miller, *Mol. Cryst. Liq. Cryst.* **1989**, *176*, 527.
[33] T. Hascall, V. Beck, S. Barlow, A. R. Cowley, D. O'Hare, *Organometallics* **2004**, *23*, 4265.
[34] J. C. Smart, B. L. Pinsky, *J. Am. Chem. Soc.* **1977**, *99*, 956.
[35] T. J. Katz, N. Acton, J. McGinnis, *J. Am. Chem. Soc.* **1972**, *94*, 6205.
[36] The oxidised Co species appear to be stable in THF on this timescale as their electronic spectra may be observed unchanged after about 30 minutes.
[37] W. H. Morrison, S. Krogsrud, D. N. Hendrickson, *Inorg. Chem.* **1973**, *12*, 1998.
[38] F. Barriere, N. Camire, W. E. Geiger, U. T. Mueller-Westerhoff, R. Sanders, *J. Am. Chem. Soc.* **2002**, *124*, 7262.
[39] S. W. Benson, *J. Am. Chem. Soc.* **1958**, *80*, 5151.
[40] F. Ammer, J. M. Savéant, *J. Electroanal. Chem.* **1973**, *47*, 215.
[41] R. Rulkens, A. J. Lough, I. Manners, S. R. Lovelace, C. Grant, W. E. Geiger, *J. Am. Chem. Soc.* **1996**, *118*, 12683.
[42] D. O. Cowan, P. Shu, F. L. Hedberg, M. Rossi, T. J. Kistenmacher, *J. Am. Chem. Soc.* **1979**, *101*, 1304.
[43] V. V. Dement'ev, F. Cervantes-Lee, L. Parkanyi, H. Sharma, K. H. Pannell, M. T. Nguyen, A. F. Diaz, *Organometallics* **1993**, *12*, 1983.

[44] D. A. Foucher, C. H. Honeyman, J. M. Nelson, B. Z. Tang, I. Manners, *Angew. Chem.* **1993**, *105*, 1843; *Angew. Chem. Int. Ed. Engl.* **1993**, *32*, 1709.

[45] H. A. Fogarty, D. L. Casher, R. Imhof, T. Schepers, D. W. Rooklin, J. Michl, *Pure Appl. Chem.* **2003**, *75*, 999.

[46] D. A. Foucher, B. Z. Tang, I. Manners, *J. Am. Chem. Soc.* **1992**, *114*, 6246.

[47] Photoinduced charge-transfer experiments have shown electronic coupling in a series of organic donor–acceptor complexes to be greater through a CMe_2-bridge than through $SiMe_2$. See C. A. van Walree, M. R. Roest, W. Schuddeboom, L. W. Jenneskens, J. W. Verhoeven, J. M. Warman, H. Kooijman, A. L. Spek, *J. Am. Chem. Soc.* **1996**, *118*, 8935.

[48] T. J. Meyer, *Acc. Chem. Res.* **1978**, *11*, 94.

[49] S. Barlow, H. E. Bunting, C. Ringham, J. C. Green, G. U. Bublitz, S. G. Boxer, J. W. Perry, S. R. Marder, *J. Am. Chem. Soc.* **1999**, *121*, 3715.

[50] S. Barlow, L. M. Henling, M. W. Day, W. P. Schaefer, J. C. Green, T. Hascall, S. R. Marder, *J. Am. Chem. Soc.* **2002**, *124*, 6285.

[51] M. J. Powers, T. J. Meyer, *J. Am. Chem. Soc.* **1978**, *100*, 4393.

[52] Limiting values of 3.92 and 5.21 Å were chosen for a_1; these are estimated as the radii of spheres that would enclose a complete $[Fe(Cp)_2]$ and $[Fe(Cp^*)_2]$ unit respectively (based on the respective Fe−H distances from the structure of **FeC** plus a value of 1.2 Å representing the H Van der Waals radius). Values for a_2 employed were 0.04 Å greater than these, representing the average change in bond length upon oxidation (see ref. [5]).

[53] I. Manners, *Chem. Commun.* **1999**, 857.

[54] M. J. Drewitt, S. Barlow, D. O'Hare, J. M. Nelson, P. Nguyen, I. Manners, *Chem. Commun.* **1996**, 2153.

[55] U. Koelle, B. Fuss, M. Belting, E. Raabe, *Organometallics* **1986**, *5*, 980.

[56] I. E. Nifant'ev, V. L. Yarnykh, M. V. Borzov, B. A. Mazurchik, V. I. Mstyslavsky, V. A. Roznyatovsky, N. A. Ustynyuk, *Organometallics* **1991**, *10*, 3739.

[57] H. Kopf, N. Klouras, *Chem. Scr.* **1983**, *22*, 64.

[58] K. C. Frisch, *J. Am. Chem. Soc.* **1953**, *75*, 6050.

[59] H. P. Fritz, C. G. Kreiter, *J. Organomet. Chem.* **1965**, *4*, 313.

[60] M. Kumada, T. Kondo, K. Mimura, M. Ishikawa, K. Yamamoto, S. Ikeda, M. Kondo, *J. Organomet. Chem.* **1972**, *43*, 293.

[61] I. Chavez, A. Alvarez-Carena, E. Molins, A. Roig, W. Maniukiewicz, A. Arancibia, V. Arancibia, H. Brand, J. M. Manriquez, *J. Organomet. Chem.* **2000**, *601*, 126.

[62] C. J. O'Conner, *Prog. Inorg. Chem.* **1982**, *29*, 203.